Drug Delivery and Translational Research (2020) 10:801–814
https://doi.org/10.1007/s13346-020-00716-5

ORIGINAL ARTICLE

Integrated nanovesicular/self-nanoemulsifying system (INV/SNES) for enhanced dual ocular drug delivery: statistical optimization, in vitro and in vivo evaluation

Carol Yousry[1] · Pakinam M. Zikry[2] · Heba M. Salem[3] · Emad B. Basalious[1] · Omaima N. El-Gazayerly[1]

Published online: 27 January 2020

Abstract

Ocular drug administration is usually problematic and suffers low bioavailability due to several physiological and biological factors that hinder their effective treatment. Terconazole (TZ) is considered as one of the effective ocular antifungal agents that is usually administrated intravitreally for higher efficacy. The aim of the work in this study is to formulate a TZ-loaded ocular drug delivery system with high efficiency and good tolerability. First, TZ-loaded bile-based nanovesicles (BBNV) were prepared and the formulation variables (namely, Span 60, cholesterol, and sodium deoxycholate levels) were optimized based on the results of the entrapment efficiency (EE%), particle size (PS), and zeta potential (ZP) using Box-Behnken statistical design. The optimized system was formulated using 73.59 mg Span 60, 1.28 mg cholesterol, and 3.11 mg sodium deoxycholate. The formulated system showed vesicles with PS of 526 nm, −42.2 mV ZP, and 93.86% EE%. TZ release, cellular uptake, and cytotoxicity of the optimized system were evaluated in vitro. In addition, in vivo assessment of its safety was conducted histopathologically and via ocular irritation test to ensure the ocular tolerance of the system. Afterwards, the optimized TZ-loaded BBNV was integrated into a self-nanoemulsifying system (SNES) to allow faster TZ release for immediate antifungal effect, enhanced ocular residence, and improved ocular permeation. TZ release study revealed more than 2 folds increment in drug release rate from the integrated system compared to BBNV alone. Finally, this integrated system was assessed for its antifungal activity in vivo where it demonstrated higher antifungal activity against induced *Candida albicans* infection.

Keywords Bilosomes · Terconazole · *Candida albicans* · Cellular uptake · Histopathology · Ocular

✉ Carol Yousry
carol.yousry@pharma.cu.edu.eg

Pakinam M. Zikry
pakinam.zikry1@gmail.com

Heba M. Salem
dr.hebasalem@cu.edu.eg

Emad B. Basalious
emad.basalious@pharma.cu.edu.eg

Omaima N. El-Gazayerly
omaima.naim@pharma.cu.edu.eg

[1] Department of Pharmaceutics and Industrial Pharmacy, Faculty of Pharmacy, Cairo University, Kasr El-Aini, Cairo 11562, Egypt

[2] Department of Pharmaceutics, Faculty of Pharmacy, October University for Modern Sciences and Arts (MSA), October City, Egypt

[3] Department of Poultry Diseases, Faculty of Veterinary Medicine, Cairo University, Giza square, Giza, Egypt

Introduction

Trauma is the most common predisposing factor for ocular fungal infections; other risk elements maybe septicemia, acquired immune deficiency syndrome (AIDS), excessive use of immunosuppressive agents, or systemic disseminated infection [1, 2]. Different regions of the eye are susceptible sites for fungal infections: eyelids, conjunctiva, lacrimal apparatus, cornea, and retina. Among all, ocular infection affecting the retina (retinitis) is considered the most devastating one [3]. *Candida albicans* is one of the most predominant causative agent for such ocular infections causing fungal chorioretinitis, a case where there is inflammation of the choroid (thin pigmented vascular coat) and retina of the eye [4]. Many studies have been done to understand the different antifungal agents and enhance their effect [5]. Among all, the azole class is emerging rapidly and is considered the best choice for treating both localized and systemic infections. This class

varies according to the number of the nitrogen atoms in their azole ring, where triazoles showed broader spectrum of applications than imidazoles. Thus, it has been the prime choice in many pharmaceutical industries [6]. Terconazole (TZ) is a triazole ketal potent antifungal drug with a wide range of activity on yeasts and fungi in vitro. It prevents *Candida albicans* transformation into its mycelium form where it interacts with cytochrome P-450 in the yeast and fungal membranes, inhibits its function which affects the membrane permeability and membrane-bound enzymes, and finally inhibits fungal growth [7]. In vivo, TZ has shown to be effective in topical treatment of dermatophytosis and candidiasis without detected side effects [8]. Also, it has been reported that intravitreal injection containing TZ is safe to the rabbit eye [9].

Topical eye drops are the most preferred form for ocular drug administration, accounting for about 90% of the ophthalmic formulations as they offer high patient compliance and cost affordability [10]. However, they suffer from the insufficient duration of drug effect owing to its low bioavailability (about only 5%). This low bioavailability can be explained in the light of the rapid and extensive pre-corneal loss due to quick tear turnover, drainage through the nasolacrimal duct, drug metabolism by anterior segment enzymes, and presence of cornea and conjunctiva epithelial cells as barriers [4, 11]. Significant efforts have been made to improve ocular bioavailability of drugs by enhancing their corneal permeation and increasing their residence time. Colloidal drug delivery systems such as nanoparticles, nanoemulsions, and liposomes have gained much attention in enhancing ophthalmic drug administration either topically or systemically [12]. Nanovesicles are novel drug delivery systems with small particle size and narrow size range showing prolonged ocular residence time thus ensuring adequate bioavailability, low irritation, and high compatibility with ocular tissues [11]. Bile-based nanovesicles (bilosomes; BBNV) are nanovesicular carriers assigning non-ionic amphiphiles in a bilayer, in addition to bile salts [13]. BBNV can improve the ocular permeation of poorly soluble drug due to its elastic properties as well as increasing its residence time [14].

The aim of the work in this study was to formulate TZ-loaded nanovesicle system with high ocular residence time, high ocular permeation, and sustained release profile for reduced dosing frequency. Thus, TZ-loaded BBNV was prepared and the influence of different formulation variables on the encapsulation efficiency (EE%), particle size (PS), and zeta potential (ZP) was statistically studied and optimized using Box-Behnken statistical design. The cytotoxicity, cellular uptake, ocular tolerance, and TZ release from the optimized system were evaluated to ensure the safety and efficacy of the formulated nanovesicles. Furthermore, the optimized system was integrated into a self-nanoemulsifying system (SNES) to modify the dispersion characteristics, improve TZ release, and enhance ocular residence and permeability. Finally, in vivo study of the integrated system was performed to compare the efficiency of the integrated system to TZ suspension.

Materials and methods

Materials

Terconazole (TZ) was supplied as a gift from Marcyrl Pharmaceutical Industries (Cairo, Egypt). Sodium deoxycholate (SDC) was purchased from BASF Co. (Florham Park, New Jersey, USA). Cholesterol, Span 60, and chloroform were purchased from Sigma-Aldrich Chemical Co. (St. Louis, Missouri, USA). Labrafil® M 2125 CS and Transcutol® HP were kindly donated by Gattefosse (Lyon, France). Sodium dihydrogen phosphate was obtained from Merck (Darmstadt, Germany). Isopropyl alcohol, methanol, sodium hydroxide, sodium lauryl sulfate, and Tween® 80 were obtained from Adwic, El-Nasr Pharmaceutical Chemicals Co. (Cairo, Egypt). All reagents and solvents used in this study were of analytical grade.

Preparation of TZ-loaded BBNV

TZ-loaded BBNV were prepared utilizing thin film hydration (TFH) technique [15]. In order to optimize the formulation process variables, Box-Behnken design was adopted to evaluate the influence of the main effects as well as the interaction between the independent variables. The selected independent variables under study were the amount of Span 60 (X1), cholesterol (X2), and bile salt (SDC; X3). The low and high level of these variables was set to 60 and 100 mg for Span 60, 0 and 20 mg for cholesterol, and 0 and 10 mg in case of SDC. Design-Expert® software (Version 7.0.0, Stat-Ease Inc., Minneapolis, USA) was used to suggest different runs with different combinations of the independent variables as shown in Table 1.

On the other hand, physicochemical properties such as entrapment efficiency (EE%, Y1), particle size (PS, Y2), polydispersity index (PDI, Y3), and zeta potential (ZP, Y4) of the prepared TZ-loaded BBNV were evaluated as the dependent variables.

Briefly, 10 mg of TZ with different amounts of Span 60 and cholesterol was dissolved in 10 mL chloroform/methanol mixture (2:1) in a round bottom flask using an ultrasonic bath sonicator (Elmasonic S, Model SH 150-41; USA) for 10 min. The obtained organic solution was evaporated under reduced pressure using a rotary evaporator for 30 min at 65 °C and 90 rpm (Rotavapor; Heidolph VV 2000, Burladingen, Germany) until a thin dry film was formed inside the flask. This dry film was then hydrated with 10 mL distilled water containing sodium deoxycholate (SDC) as the bile salt, by

Table 1 Composition of TZ-loaded BBNV, independent variables, and measured responses of Box-Behnken statistical design

Run	X_1: Span	X_2: cholesterol	X_3: SDC	Y_1: EE ± SD % w/w	Y_2: PS ± SD nm	Y_3: PDI ± SD	Y_4: ZP ± SD mV	Drug content mg/mL
1	80	10	5	84.00 ± 0.51	699.80 ± 44.97	0.16 ± 0.02	− 45.40 ± 0.00	1.00 ± 0.00
2	80	0	10	67.79 ± 1.20	478.20 ± 12.87	0.66 ± 0.06	− 48.20 ± 0.42	1.00 ± 0.01
3	60	0	5	64.09 ± 0.83	489.00 ± 89.10	0.83 ± 0.06	− 33.40 ± 0.99	0.98 ± 0.03
4	80	10	5	83.00 ± 0.91	851.30 ± 67.18	0.20 ± 0.14	− 43.00 ± 2.83	1.00 ± 0.08
5	80	20	10	84.05 ± 1.41	999.00 ± 02.55	0.78 ± 0.07	− 52.60 ± 0.99	0.98 ± 0.02
6	100	20	5	86.39 ± 0.93	695.00 ± 20.22	0.92 ± 0.12	− 45.50 ± 0.42	1.00 ± 0.00
7	80	10	5	84.50 ± 1.41	708.90 ± 30.55	0.20 ± 0.03	− 48.90 ± 0.42	0.98 ± 0.01
8	80	0	0	72.47 ± 0.21	677.10 ± 20.22	0.96 ± 0.05	− 33.90 ± 0.57	0.98 ± 0.03
9	60	10	10	85.64 ± 1.62	666.50 ± 15.84	0.31 ± 0.01	− 51.90 ± 0.00	0.98 ± 0.01
10	80	20	0	70.68 ± 0.17	878.00 ± 29.98	1.00 ± 0.00	− 40.20 ± 0.14	0.99 ± 0.01
11	100	10	0	60.64 ± 3.64	779.00 ± 04.24	0.59 ± 0.06	− 34.70 ± 1.13	0.98 ± 0.04
12	80	10	5	84.00 ± 0.91	873.60 ± 37.34	0.20 ± 0.05	− 52.10 ± 0.42	1.00 ± 0.07
13	100	10	10	75.84 ± 0.73	957.90 ± 201.7	0.41 ± 0.01	− 51.90 ± 0.00	0.99 ± 0.01
14	80	10	5	82.55 ± 0.16	709.30 ± 13.01	0.15 ± 0.00	− 43.50 ± 0.85	0.99 ± 0.03
15	60	20	5	83.93 ± 1.46	621.80 ± 13.44	0.13 ± 0.02	− 43.10 ± 0.42	1.00 ± 0.03
16	100	0	5	66.53 ± 2.70	659.60 ± 202.7	0.98 ± 0.02	− 34.80 ± 0.57	0.99 ± 0.00
17	60	10	0	60.00 ± 0.86	476.90 ± 30.83	0.81 ± 0.01	− 45.00 ± 0.00	0.99 ± 0.01

rotating the flask in a water bath maintained at 65 °C for 1 h under normal pressure to form a crude dispersion of TZ-loaded BBNV. Finally, the formulated BBNV dispersion was sonicated for 5 min in a bath sonicator at 25 °C to reduce the particle size of the vesicles and stored at 4 °C for characterization [16].

In vitro characterization of TZ-loaded BBNV

Total drug content

One milliliter of the formulated BBNV aqueous dispersion was diluted with isopropyl alcohol and sonicated for 5 min to allow the complete disruption of the formulated vesicles. The resulted clear solution was measured spectrophotometrically at 297 nm (UV Spectrophotometer 2401/PC; Shimadzu, Japan) and TZ content was calculated [4].

Drug entrapment efficiency (EE%)

For all of the prepared systems, TZ-loaded BBNV were separated from the aqueous dispersion by centrifugation (Heraeus Megafuge 16R; ThermoFisher Scientific, Germany) at 12,000 rpm for 1 h at 4 °C and the residue was washed twice with water to remove the excess unentrapped TZ. The separated vesicles were diluted with isopropyl alcohol and sonicated for 5 min until a clear solution is obtained. Finally, the solution was measured spectrophotometrically at 297 nm and TZ entrapment was calculated according to the following equation [17]:

$$EE\% = \frac{amount\ of\ the\ entrapped\ TZ}{total\ amount\ of\ TZ} x\ 100 \quad (1)$$

The individual values for two replicates were determined and their mean values were reported.

Particle size (PS), polydispersity index (PDI), and zeta potential (ZP)

The PS and PDI of all the formulated BBNV systems were determined by Malvern Zetasizer Nanoseries (Nano ZS; Malvern Instruments, UK) adopting the dynamic light-scattering technique. PDI values are a valuable indication for the size distribution uuniformity, where small values (around 0) reveal a homogenous and uniform size distribution, while larger PDI values (around 1) reflect a higher heterogeneity [18]. ZP measurement was carried out using the same instrument by observing the electrophoretic mobility of the particles in an electrical field. The dispersions were properly diluted with distilled water before measurement [3]. All measurements were performed in duplicate and their mean values were reported.

Statistical analysis and optimization of the formulation

Statistical analyses via analysis of variance (ANOVA) to identify the influence of the independent variables on the dependent variables were performed using Design-Expert® software adopting Box-Behnken design. The base design

consisted of 17 runs and the p value < 0.05 was considered to be statistically significant. The suitable models for Box-Behnken design include linear, two-factor interaction, and quadratic models. These models have provided several comparative measures for model selection. Predicted R^2 (multiple correlation coefficient), which gives a correlation between experimental response and predicted response, should be high for any model to be significant. Adjusted R^2 (adjusted multiple correlation coefficient) gives a similar correlation but after ignoring the insignificant model terms, and should show good agreement with predicted R^2 for the model to be fit [19]. Afterwards, the dependent variables' results were statistically optimized to select the most desirable system where the optimization criteria were set to EE% (Y1) > 70% w/w, PS (Y_2) < 600 nm, PDI (Y_3) < 0.7, and ZP (Y_4) < − 30 mV. The optimized system was formulated, characterized, and used in further studies.

Evaluation of the optimized BBNV system

Cytotoxicity test

The cytotoxicity of the optimized BBNV system (containing TZ in 1 mg/mL) was evaluated using normal human primary corneal epithelial cell line which were obtained from American Type Culture Collection (ATTCC® PCS700010™). Drug suspension (1 mg/mL) and drug solution (1 mg/mL; drug dissolved in phosphate buffer pH 7.4 containing 1% sodium lauryl sulfate (SLS)) were also performed for comparison. Cells were cultured under standard conditions (5% CO_2, 98% humidity, 37 °C) in medium supplemented with 10% heat-inactivated fetal bovine serum (FBS), penicillin (100 units/mL), streptomycin (100 μg/mL), L-glutamine (0.3 mg/mL), pyruvic acid (0.11 mg/mL), 0.37% $NaHCO_3$, and 50 μM of 2-mercaptoethanol. Hundred microliter growth medium (at a density of 1.2–1.8 × 10,000 cells/well) were incubated for 24 h in 96-well plates with different serial dilution (100, 10, 1, 0.1, 0.01 μg/mL) of each of the optimized system, drug suspension, and drug solution. The incubated wells were rinsed three times using phosphate buffer saline (PBS), then 50 μL of MTT reagent (3-(4,5-dimethylthiazol-2-yl)-2,5-diphenyltetrazolium bromide) was added in each well and incubated for 4 h at room temp in dark area. Afterwards, plates were centrifuged at 200×g and supernatant was aspirated. Finally, 100 μL of dimethyl sulfoxide (DMSO) was added to dissolve the MTT formazan crystals and the optical density (OD) of the wells was measured at wavelength 570 nm (against background wavelength 690 nm) on ELISA plate reader (Thermo Labs, USA). The optical density of the violet color of MTT formazan crystals is directly related to the cell viability. Cell viability was calculated by comparing the absorbance of the treated wells against the untreated ones and a relation was constructed between the different concentrations of each tested system against the percentage viability of the cells where IC50 for each system was finally anticipated [12, 13].

Cellular uptake study

Normal human primary corneal epithelial cornea cell line (PCS700010™) was seeded in 48-well plates, incubated overnight at 37 °C with 100 μL growth medium (Roswell Park Memorial Institude (RPMI-1640) media, 10% FBS, and 1% antimycotic antibiotic mixture). The optimized BBNV system was diluted and incubated with the culture medium at 37 °C for 24 h (at a final concentration of 2.7 μg/mL which is equivalent to 5 μM TZ). Afterwards, 100 μL was withdrawn from each well to detect the extracellular amount of TZ using HPLC. On the other hand, the remaining cells were washed three times with sterile PBS to remove any excess unentrapped drug. Trypsinization of cells was performed by addition of trypsin which was then diluted in 50 μL growth media and vortexed for 2 min. Freeze–thaw cycle technique was performed for all the wells to allow cell lysis and the final dispersion was centrifuged for 30 min at 14,000 rpm. The intracellular TZ was quantitively detected in the supernatant using HPLC. Drug suspension was also performed for comparison.

In vivo safety assessment

Three male albino rabbits (2–2.5 kg) were assigned for evaluating the ocular irritation and ophthalmic histopathological effect of the optimized TZ-loaded BBNV system.

The rabbits were housed according to the National Institute of Health guidelines. In addition, handling of the animals and all their biological tissues were performed in accordance with the regulations of Research Ethics Committee for experimental and clinical studies at Faculty of Pharmacy, Cairo University (REC-FOPCU; PI (1051)), and guidelines of Association for Research in Vision and Opthalmology (ARVO) resolution (Rockville, MD, USA). Both eyes were visually inspected before testing to ensure the absence of any defects. One drop (0.1 mL) of the optimized BBNV system was instilled into one eye while physiological saline solution was instilled in the contralateral eye as a control. The instillation was repeated every hour for a period of 6 h.

Ocular tolerance testing

Both eyes of rabbits were visually examined using a slit lamp to detect any irritation signs, such as conjunctivitis, corneal edema, and/or hyperemia. Their response to the applied system was evaluated according to Draize scoring technique [20], where system was concluded to be non-irritant if it showed score range from 0 to 3.9, slightly irritant in range of 4 to 8.9,

moderately irritant in case of 9 to 12.9 range, and seriously irritant from 13 to 16.

Histopathological examination Thirty minutes after the last instillation, rabbits were euthanized by intravenous injection of sodium pentobarbital overdose. Both corneas, the one receiving the optimized BBNV system and the control cornea receiving physiological saline, were isolated, rinsed in physiological saline, and subsequently fixed in 10% formalin for 24 h. Afterwards, the isolated corneas were washed with tap water, and then serial dilutions of alcohol (methanol, ethanol, and absolute ethanol) were used for dehydration. Specimens were cleared in xylene and embedded in paraffin at 56 °C in hot air oven for 24 h. Using sledge microtome, paraffin beeswax tissue blocks were prepared by sectioning at 4 μm thickness. The obtained tissue sections were collected on glass slides, deparaffinized, and stained by hematoxylin and eosin stain in order to be examined under the light electric microscope [1].

Formulation of self-nanoemulsifying system containing terconazole

Based on the previous results, TZ-loaded self-nanoemulsifying system (SNES) was prepared and integrated with the previously optimized TZ-loaded BBNV. SNES is known to enhance ocular permeability and promote drug release [21, 22]. Preliminary drug solubility studies for screening different oils, surfactants, and co-surfactants were performed and different systems were prepared and optimized [23]. The optimized system was formulated of Labrafil® M 2125 CS as the oily component, Tween® 80 as a surfactant, and Transcutol® HP as co-surfactant/co-solvent in ratios of 20:50:30, respectively. TZ was vortexed (Stuart SA8; UK) in Tween® 80 and Transcutol® HP for 2 min. Labrafil® M 2125 CS was then added into the mixture and vortexed again until a homogenous clear solution of concentration 1 mg/mL was obtained which was then kept at 25 °C in tightly closed glass bottles to be subjected to further studies [3, 18]. The globule size and PDI of the formulated TZ-loaded SNES were measured as discussed before.

Preparation of integrated nanovesicular/self-nanoemulsifying system containing terconazole (INV/SNES)

In our study, an integrated system (INV/SNES) with a total concentration of 2 mg TZ/mL was prepared by dispersing BBNV residue equivalent to 1 mg TZ (for a sustained release target) in 1 mL of SNES containing 1 mg TZ (for immediate TZ release). TZ-loaded BBNV was separated from the unentrapped TZ in the dispersion by centrifugation and the seperated BBNV residue was redispersed in the SNES by votexing. The drug content of the formulated integrated system was measured as previously mentioned.

Characterization of the integrated system

In vitro dispersibility study An in vitro dispersibility study was done to observe the self-emulsification efficiency of INV/SNES [24]. One drop of the INV/SNES was added to 10 mL of phosphate buffer (pH 7.4) in a glass tube. The time required for complete dispersion of the INV/SNES was determined.

Transmission electron microscopy The size and surface topography of the optimized BBNV system as well as the INV/SNES was observed using transmission electron microscopy (TEM) operating at 80 kV (JEM-1230, Jeol,Tokyo, Japan). A single drop of diluted dispersion was deposited on the surface of a carbon-coated copper grid, which was then negatively stained with 2% phosphotungstic acid and allowed to dry at room temperature for investigation [17].

In vitro release studies The release of TZ from the integrated system (INV/SNES) was observed using a drug dissolution tester with slight modification. In addition, TZ release from the optimized BBNV dispersion and its residue (obtained after centrifugation of the prepared dispersion and removal of excess unentrapped TZ) as well as the selected SNES (1 mg/mL) was performed for comparison. An accurate amount of any of the formulated system, equivalent to 2 mg TZ, was placed in a glass cylinder based with membrane filter (Nylon, 0.22 μm, 47 mm) which was then fitted to the shaft of the dissolution tester (Apparatus 1), operated at 37 °C, 50 rpm for 24 h against 250 mL of phosphate buffer (pH 7.4) containing 1% SLS as the receiving release medium. Aliquots of 3 mL sample were withdrawn at predefined time points for the release duration (0.5, 1, 2, 4, 6, 20, 22, and 24 h) and were replenished with equal volume of fresh release medium. TZ concentration in each sample was quantitatively determined using a previously validated HPLC method (Waters Alliance HPLC system, Milford, *Massachusetts*, USA) installed with Zorbax eclipse C_{18} column (250 × 4.6 mm, 5 μm). A 100-μL sample was injected at 45 °C where TZ was eluted using acetonitrile:0.01 M ammonium acetate buffer (55:45, v:v) as mobile phase at flow rate of 1.5 mL/min and measured at wavelength 220 nm. The in vitro drug release studies were performed in duplicates.

In vivo evaluation of the INV/SNES antifungal efficacy

Animals

Twelve male rabbits, weighing approximately 2.5 kg each, were used in this study. The use and handling of the animals

in this study were performed in compliance with the ARVO statement and approved by the REC-FOPCU (PI(1051)). Initially, the rabbits were investigated to detect any signs of ocular pathology.

Inoculation technique

Candida albicans (ATCC® 18804) was used to promote ocular fungal infection via surface inoculation for the in vivo evaluation of the tested INV/SNES system. Rabbits were sedated by intraperitoneal injection of 0.5 mL thiopental. All rabbits received immunosuppresant drug (0.1 mL dexamethasone into each eye) before inoculation to enhance the fungal infection [25]. Intrastromal injection of 10 μL inoculum (*Candida albicans*, containing 2.5×10^5 cells) was introduced in both eyes of rabbits by inserting a sterile 27-gauge needle into the central corneal stroma tangential to the corneal surface to a depth of one half of the corneal thickness. Rabbits were excluded from the study if any penetration of the inoculum into the anterior chamber or reflux of the inoculum was observed. After 48 h of inoculation, treatments were instilled into the conjunctival sac of rabbits [26].

Treatment technique

The rabbits were randomly assigned into three different groups: group one received INV/SNES (2 mg/mL), group two received drug suspension (2 mg/mL), and group three received physiological saline solution only as control.

One drop (50 μL) of each treatment containing 0.1 mg drug was instilled in both eyes two times daily (every 12 h) until clinical recovery was fully observed [26]. Photographs were taken before and after induction of keratitis as well as after full recovery to detect signs of improvement. At the end of the study, aqueous humor were collected from groups 1 and 2 and were cultivated on agar medium to detect the microbiological count of *Candida albicans*.

Results and discussion

BBNV was formulated to enhance ocular TZ delivery as an antifungal agent with high percent yield (91.20–97.80%). The bile salt incorporation in the system allows flexible vesicle formulation which may improve ocular retention and permeation. Box-Behnken statistical design was performed to optimize TZ-loaded BBNV systems and to conclude mathematical equations correlating the previously mentioned independent formulation variables with the different dependent responses of TZ-loaded BBNV systems as shown in Table 2. The approximation of response values of the EE% (Y_1) and PDI (Y_3) based on the quadratic model was the most suitable because it showed high values for R^2, as well as good agreement for the adjusted and predicted values of R^2, while the linear model was selected for the approximation of response values of the particle size (Y_2) and zeta potential (Y_4). It can be observed that the values of predicted R^2 and adjusted R^2 are in good agreement resulting in a reliable model. The initial model was refined by including in the model only those terms for which the level of significance was below or equal to $p \leq 0.05$.

In vitro characterization of all the prepared systems

Total drug content

All the prepared BBNV dispersions showed acceptable TZ content relative to the initially added amount (1 mg/mL) where drug content of all the systems ranged from 98 to 100% w/w.

Entrapment efficiency % (EE%)

The formulated BBNV systems showed high entrapment efficiency of TZ ranging from 60 to 86.39% (w/w) as represented in Table 1. ANOVA statistical analysis of the results suggested the quadratic model is the model of choice for the statistical study of the data. The quadratic model revealed that the added amount of cholesterol (X_2) and sodium deoxycholate (X_3) as well as the interaction between them had a significant effect on the EE% ($p < 0.05$) (Fig. 1a). Increasing cholesterol level to the formulation at high/low level of SDC resulted in vesicles with higher EE%. This could be attributed to the increase in the bilayer rigidity of BBNV upon increasing cholesterol level as previously reported by Khan and Irchhaiya [27]. On the other hand, increasing SDC level from 0 to 5 mg at high/low level of cholesterol resulted in an increase in the EE% of the formulated vesicles whereas further increment in SDC level resulted in vesicles with lower EE%. Increasing bile salt level (SDC) may enhance the membrane elasticity and drug solubilization in the bilayered membrane of the BBNV which may result in higher EE%. However; higher levels of SDC will increase drug solubilization in the external dispersion medium causing drug leakage out of the formulated system. Also, drug leakage could be augmented by the higher fluidizing effects of SDC on the lipid bilayers of the BBNV [28, 29].

PS, PDI, and ZP

Particle size, particle size distribution, and zeta potential are considered the most essential parameters while evaluating the physical stability of nanoscaled drug delivery systems. In addition, the particle size exerts a specific role in the safe and efficient ocular administration of drugs. Nanometric drug delivery systems ensure less ocular irritation and better patient

Table 2 Statistical regression values for the measured dependent responses

Response	Model	Adjusted R^2	Predicted R^2	Final equation in terms of actual factors
Y_1: EE%	Quadratic	0.9875	0.9621	$Y_1 = -60.661 + 3.0814\ X_1 + 0.3691\ X_2 + 3.6450\ X_3 + 0.1077\ X_2\ X_3 - 0.0190\ X_1^2 - 0.3289\ X_3^2$
Y_2: PS	Linear	0.4593	0.2160	$Y_2 = 143.9066176 + 5.751875\ X_1 + 9.66125\ X_2 + 2.265\ X_3$
Y_3: PDI	Quadratic	0.9551	0.8057	$Y_3 = 4.1402 - 0.0757\ X_1 - 0.1005\ X_2 - 0.1590\ X_3 + 0.0008\ X_1\ X_3 + 0.0005\ X_1^2 + 0.0050\ X_2^2 + 0.0065\ X_3^2$
Y_4: ZP	Linear	0.5436	0.3491	$Y4 = -37.018 + 0.0406\ X_1 - 0.3888\ X_2 - 1.2700\ X_3$

convenience with high improvement in corneal penetration and retention time. It was reported that particles intended for ocular administration should not exceed 10 μm in size [30].

In our study, all of the formulated TZ-loaded BBNV showed mean PS ranging between 476.9 and 999 nm (Table 1). ANOVA test for significance revealed that only Span 60 and cholesterol levels showed a positive significant effect ($p < 0.05$) on the measured PS (Fig. 1b). Increasing Span 60 level or cholesterol level resulted in vesicles with larger particle size. The increase in particle size observed with Span 60 increment could be attributed mainly to the long saturated alkyl chain (C16) of Span 60 which may result in the formation of larger vesicles [31, 32]. On the other hand, increasing PS with the additional increment of cholesterol could be a result of the increment in the width of the bilayer membrane of the formulated nanovesicles due to the incorporation of more cholesterol molecules which subsequently result in larger vesicle size [31].

Particle size distribution, as indicated by the PDI, is considered an important parameter while evaluating the homogenity of the formulated BBNV dispersion. Small PDI values (near 0) reveal more homogenous dispersion with uniform size distribution, while large PDI values (near 1) reflect heterogenous dispersion with a wide size distribution range [18]. Most of the formulated TZ-loaded BBNV showed acceptable PS distribution with PDI in the range of 0.13–0.66; only few systems showed higher unacceptable PDI range (> 0.7). ANOVA test showed that only SDC level and its interaction with Span 60 had a significant effect on the PDI results ($p < 0.05$). Increasing SDC level from 0 to 5 mg at high/low level of Span 60 resulted in BBNV system with low PDI level; however, the PDI level of the formulated vesicles was significantly increased upon further increment in SDC level (from 5 to 10 mg) (Fig. 1c). It was reported that substantial decrease in PDI of BBNV vesicles was associated with the increase of bile salts, which may be attributed to the reduction in surface tension of the vesicles and the enhancement in the bilayer flexibility [33]. However, the increament in the PDI level of the vesicles observed with further increase in the level of SDC may be related to the uneven enlargement of the vesicles and the higher viscosity of the medium that result in different vesicles' size [29, 34].

ZP is considered an indirect measure for stability of colloidal dispersions; vesicles with high surface charge are more stable against accumulation than uncharged vesicles as it hinders aggregation of vesicles [29, 35, 36]. All the formulated systems showed a negative surface charge with ZP values ranging from − 33.40 to − 52.60 mV (Table 1). ANOVA test showed that cholesterol and SDC level had a significant positive effect on ZP

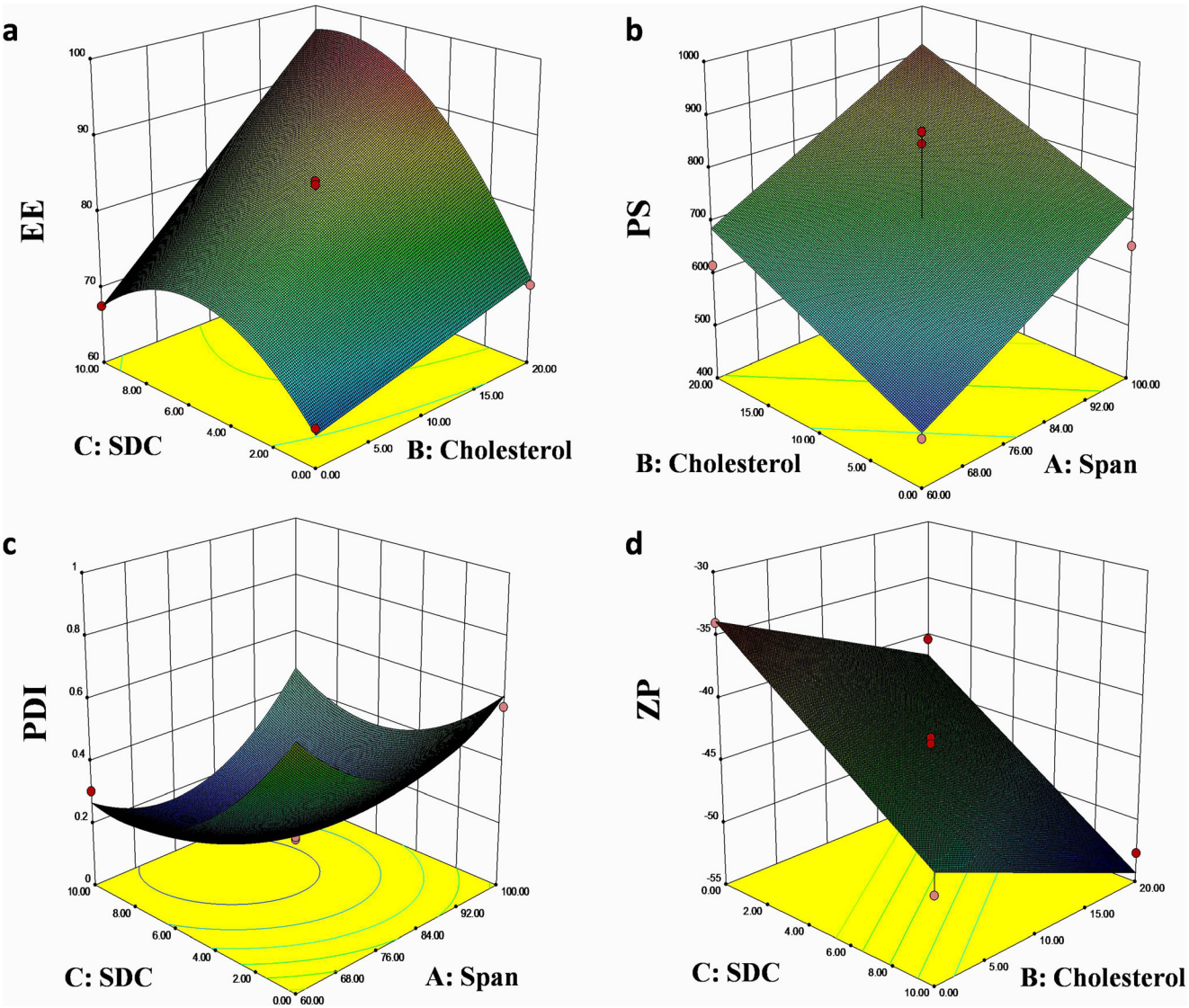

Fig. 1 Statistical surface response plot showing the effect of cholesterol and SDC level on the entrapment efficiency (EE%) (**a**), Span 60 and cholesterol level on the particle size (PS) (**b**), Span 60 and SDC level on the polydispersity index (PDI) (**c**), and cholesterol and SDC level on the zeta potential (ZP) (**d**) of TZ-loaded BBNV

($p < 0.05$), where increasing any of their levels resulted in higher ZP values (Fig. 1d). Increasing the level of SDC, a negative charge inducer, leads to an increase in the negative ZP of the formulated BBNVs as a result of its anionic nature [17, 37]. Also, increasing cholesterol level leads to slight increase in the negative ZP of the vesicles. Similar finding was observed by Jovanović et al. [38] where they found that increasing sterols' concentration leads to higher absolute zeta values. Sterols' inclusion affects the bilayer arrangement of the vesicles irrespective to the functional groups available, which may participate in the hydrogen bonding interaction with the sterols and cause changes in the total surface charge of the prepared systems. Also, increasing cholesterol level may increase the spacing between the membrane bilayer molecules allowing more space for SDC inclusion which may affect the surface zeta potential of the systems.

Statistical optimization of the formulation

Statistical optimization of all the investigated variables was performed to detect the levels of input variables from which a product with high quality may be produced. The optimization criteria was set to EE% ($Y1$) > 70% w/w, PS (Y_2) < 600 nm, PDI (Y_3) < 0.7, and ZP (Y_4) < − 30 mV. Graphical and numerical analyses using the Design-Expert® software were done based on the criterion of desirability [39] and the optimized system was selected as a compromise between the high EE%, low PS, low PDI values, and high ZP with desirability factor 1. It was composed of 10 mg drug, 73.59 mg Span 60, 1.28 mg cholesterol, and

Table 3 The predicted and observed values for the dependent variables of the optimized system suggested by Box-Behnken statistical design

Response	EE% (w/w)	PS (nm)	PDI	ZP (mV)
Predicted values	89	586.6	0.666	− 38.5
Observed values	93.86 ± 0.03	526 ± 0.00	0.767 ± 0.16	− 42.2 ± 5.59

3.11 mg sodium deoxycholate. The optimized system was prepared to confirm the validity of the optimization procedure. The predicted and observed responses of the optimized TZ-loaded BBNV are presented in Table 3. The design space is a multidimensional combination and the study of the interaction of the input variables and parameters of the process has been found to provide quality assurance [40]. Working within the design space ensures that no change is considered and nearly gives the required quality of the optimized BBNV, while working out of the design space may cause change and gives a product with low quality. The design space, represented in Fig. 2, shows the common region of successful operating ranges determined using the responses of the dependent variables. There was no proposed design space for high levels of Span 60 (more than 75 mg).

Evaluation of the optimized BBNV system

Cytotoxicity test

Cytotoxicity test revealed that IC50 for the optimized TZ-loaded BBNV system is 82.8 μM compared to 6.3 μM and 6.75 μM in case of drug solution and drug suspension, respectively, as shown in Fig. 3. This result ensures the safe administration of the optimized BBNV system as it will offer less cytotoxic effects even at higher drug concentrations.

Cellular uptake study

After 24 h incubation with human cornea cell line, the extracellular and intracellular TZ were quantitatively analyzed for both the optimized BBNV system as well as the drug suspension (Fig. 4) and percent TZ uptaken by the cells were calculated. The optimized BBNV system showed 65.86% w/w of TZ uptaken by the cells compared to 71.28% w/w in drug suspension. These results could be attributed to the long incubation period (24 h) between both systems and the cells. This long incubation period could be the main reason for the failure of this study to discriminate between the cellular uptake of the optimized BBNV and TZ suspension.

In vivo safety assessment

Ocular tolerance test Upon visual examination, the corneas treated with TZ-loaded BBNV did not show any sign of occular irritation, redness, or corneal edema and thus were scored zero according to Draize scoring system. These observations suggested high ocular tolerance to the optimized TZ-loaded BBNV to be confirmed by the histopathological study.

Histopathological study Light microscopic examination was conducted on stained sections of both control and BBNV-

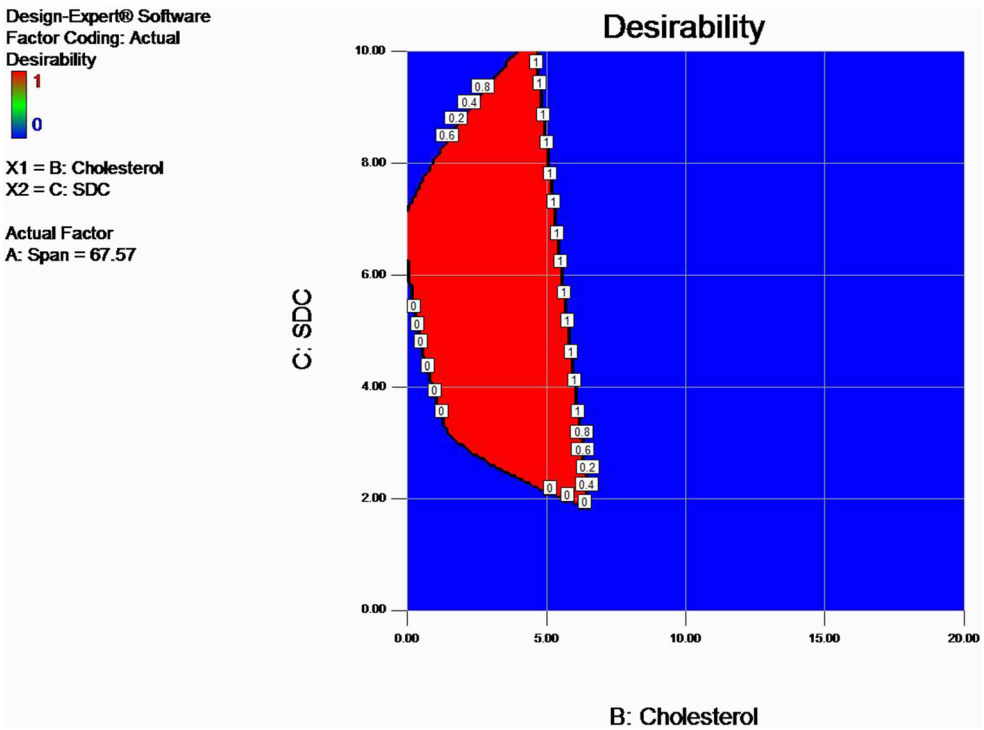

Fig. 2 The working design space as proposed by Design-Expert software, showing the common region of successful operating ranges determined using the responses of the dependent variables

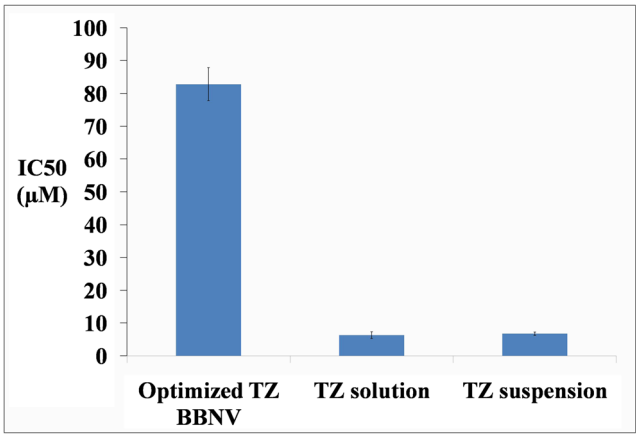

Fig. 3 Bar chart showing the inhibitory concentrations (IC50) of TZ-loaded BBNV, TZ solution, and TZ suspension after 24 h incubation with human primary corneal epithelial cell line

treated group. The examination revealed no histopathological alteration in the cornea (outer and inner lining of the epithelium and stroma in between (Fig. $5a_2$, b_2), as well as the iris (Fig. $5c_2$), retina, choroid, and sclera (Fig. $5d_2$) of the treated group when compared to the control one (Fig. $5a_1$–d_1). The absence of any ocular irritation and intolerability suggests that TZ-loaded BBNV is a well-tolerated system that can be used without toxicity concerns.

Formulation of self-nanoemulsifying system containing terconazole

SNES containing TZ was formulated to be used as vehicle for BBNV to enhance its penetration through cellular membrane, in addition; SNES allows faster drug release to be used for an immediate antifungal effect. Different oils, SAA, and co-SAA in different ratios were screened for formulation of SNES and the optimized system was selected to be composed of Labrafil® M 2125 CS, Tween® 80, and Transcutol® HP in ratios of 20:50:30, respectively.

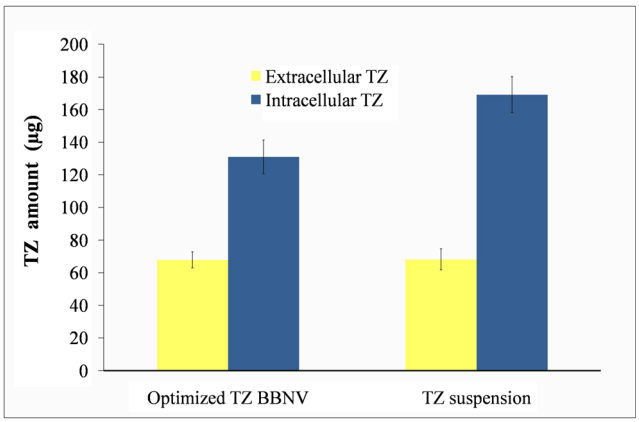

Fig. 4 Bar chart for the cellular uptake study demonstrating extracellular and intracellular TZ amount after 24 h incubation of optimized TZ-loaded BBNV with normal conea cell line compared to TZ suspension

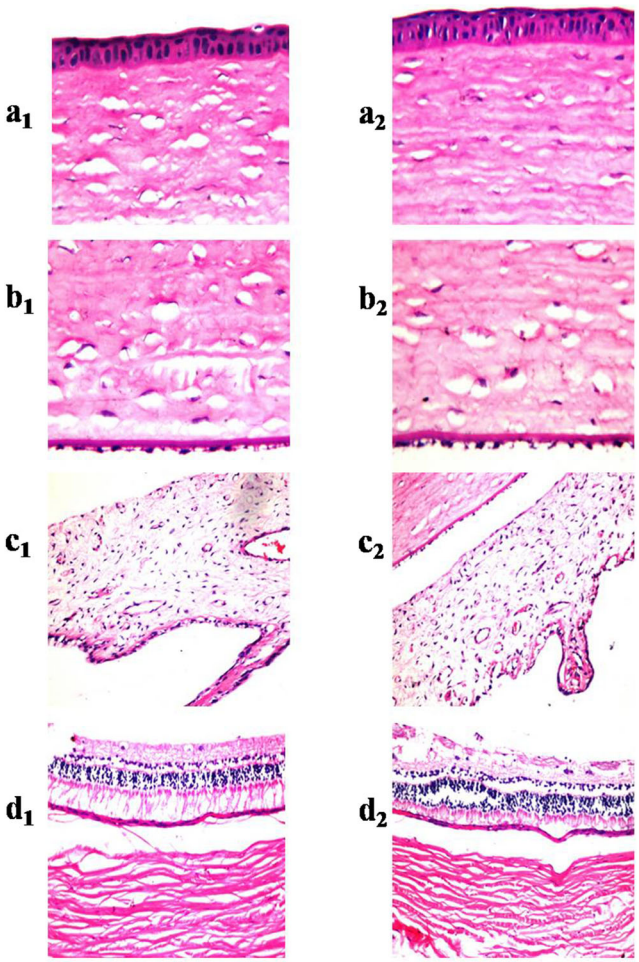

Fig. 5 Histopathological stained sections (hematoxylin and eosin) of normal untreated rabbit eye (**a1**–**d1**); and rabbit eye treated with TZ-loaded BBNV (**a2**–**d2**); where **a1** and **a2** represent the outer layer of the cornea, **b1** and **b2** represent the inner layer of the cornea both at magnification power of × 80, while **c1** and **c2** represent the iris and **d1** and **d2** represent the retina, choroid, and sclera at magnification power of × 40

Globule size is the most important criterion while evaluating the nanoemulsion stability and the major step in enhancing drug bioavailability [41]. Smaller globule size exhibits larger interfacial surface area for higher absorption and rapid drug release thus enhancing drug bioavailability [42]. The formulated TZ-loaded SNES showed small globule size of 15.13 ± 0.34 nm with 0.067 ± 0.01 PDI indicating a uniform globule size distribution.

In vitro irritation test (HET-CAM test) was conducted and the formulated system did not show any sign of irritation.

Characterization of the integrated nanovesicular/self-nanoemulsifying system (INV/SNES)

INV/SNES was formulated with a total concentration of 2 mg TZ/mL. One milligram of the drug was supplied in the form of

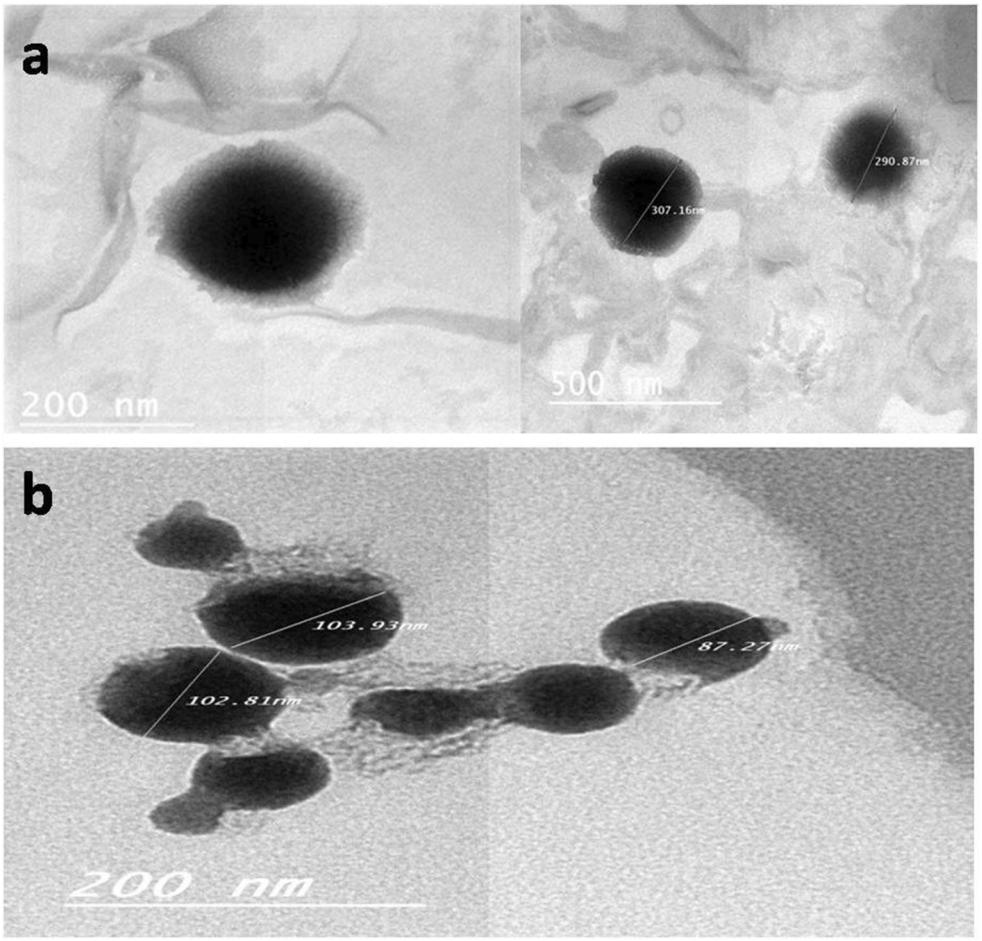

Fig. 6 Transmission electron photomicrographs showing the optimized TZ-loaded BBNV system (**a**) and the INV/SNES system (**b**)

TZ-loaded BBNV for an anticipated sustained TZ release and 1 mg was in the form of SNES for an immediate release and rapid antifungal effect. Drug content measurement of the formulated integrated system was found to be 98% w/w.

In vitro dispersibility test

The in vitro dispersibility test revealed that one drop of the INV/SNES showed complete dispersion within 2–3 s when

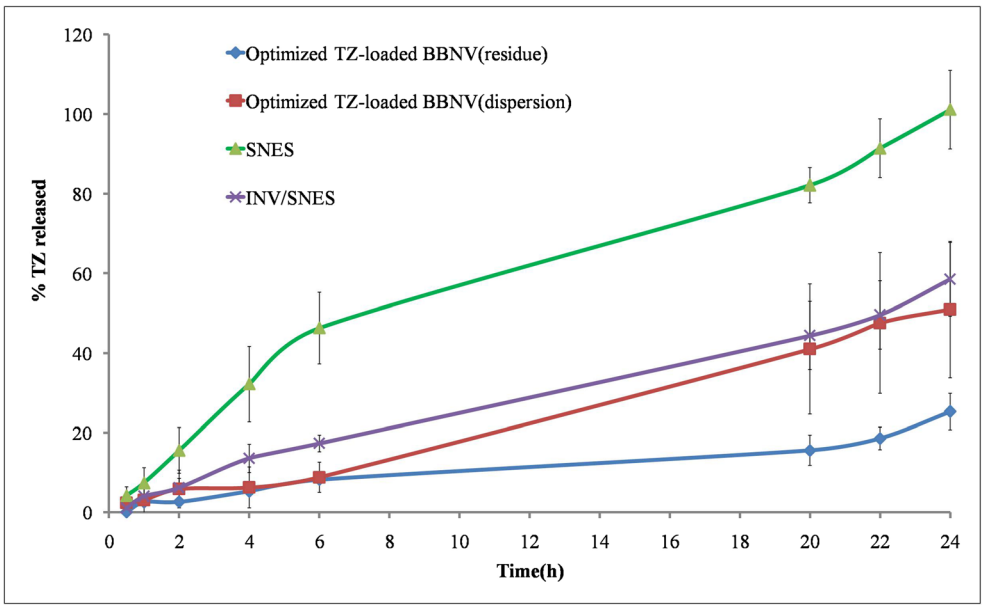

Fig. 7 In vitro release profiles showing TZ release from the optimized TZ-loaded BBNV (dispersion), the residue of the optimized TZ-loaded BBNV, SNES, INV/SNESS, and TZ suspension (each containing 2 mg TZ)

added to 10 mL phosphate buffer (pH 7.4). This finding may confirm the good dispersibility of the integrated system with the tear fluid upon application and subsequently, its good ocular tolerance.

Transmission electron microscopy (TEM)

TEM was used to explore the structure and morphology of the optimized BBNV and INV/SNES after dilution with distilled water. Figure 6a shows non-aggregating unilamellar spherical vesicles with solid dense structure of the optimized BBNV sytem. Whereas, Fig. 6b demonstrated the non-aggregating unilamellar spherical-shaped vesicles of BBNV as well as small spherical globules of SNES with no signs of coalescence. TEM also showed a significant reduction in the vesicular size upon comparing INV/SNES with the BBNV alone indicating the capability of the integrated system for higher corneal penetration.

In vitro release studies

TZ release from the optimized TZ-loaded BBNV dispersion, the whole integrated system (INV/SNES), and each of its components alone (TZ-loaded SNES and the residue of the optimized TZ-loaded BBNV system obtained after centrifugation and removal of the unentrapped TZ) are presented in Fig. 7.

The optimized TZ-loaded BBNV dispersion markedly offered sustained drug release where Q6h, Q20h, and Q24h were 8.74 ± 3.80, 41 ± 16.33, and 50.93 ± 17.15% w/w, respectively. This observed sustained release effect of the BBNV could be attributed mainly to the bilayer barrier of the vesicles surrounding TZ and hindering its release.

On the other hand, SNES demonstrated faster release profile as Q6h, Q20h, and Q24h showed percentage TZ release of about 46.29 ± 9.01, 82.15 ± 4.42, and 100 ± 9.90% w/w. This rapid release profile may count for the immediate antifungal effect required upon integration with the sustained release TZ-loaded BBNV system.

Upon studying TZ release from the integrated system (INV/SNES) and comparing it with each of its component alone, an intermediate release pattern between the slow release profile of the optimized BBNV residue and the fast release profile of SNES was observed. Q24h was found to be 25.27 ± 4.59, 100 ± 9.90, and 58.52 ± 9.25% (w/w) for BBNV residue, SNES, and INV/SNES, respectively, which indicates more than 2 folds increment in drug release rate from INV/SNES compared to the vesicular system alone. This release profile of the integrated system may suggest good antifungal activity with an immediate release pattern offered by the SNES followed by sustained release antifungal effect offered by the BBNV system.

In vivo antifungal evaluation of INV/SNES

In this study, the rabbit model was used to evaluate the antifungal efficacy of TZ treatment against *C. albicans*-induced fungal keratitis.

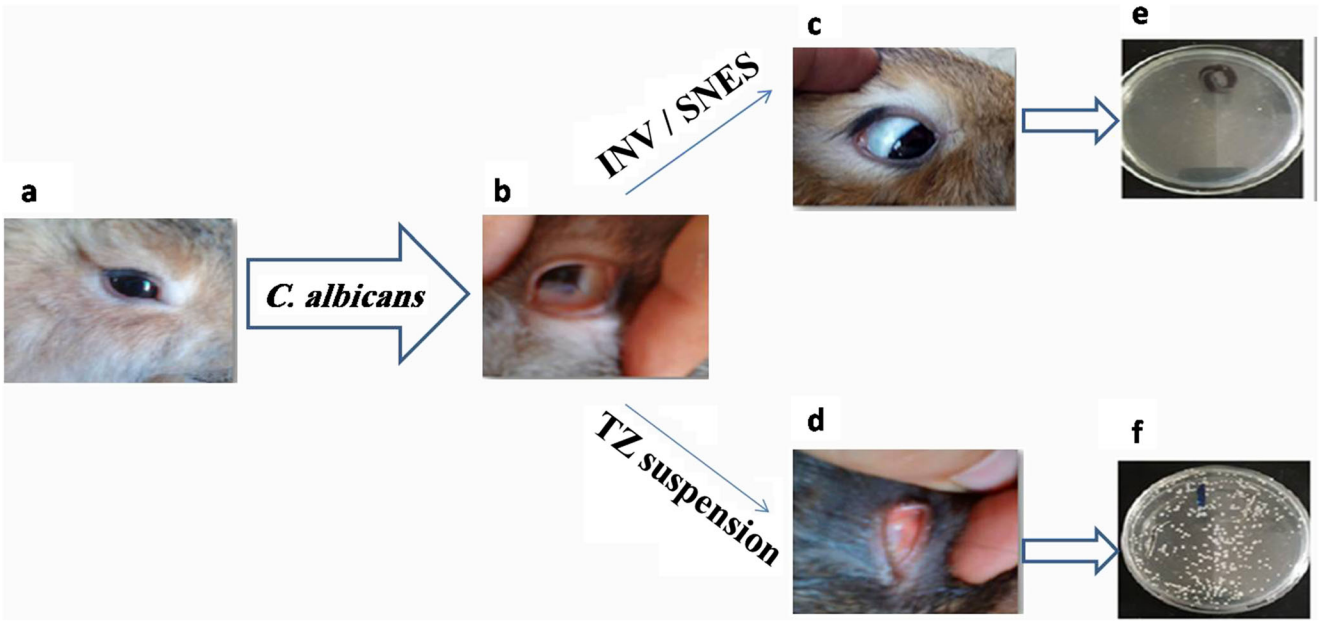

Fig. 8 Photographic images showing normal rabbit eye (**a**), rabbit eye after infection with *Candida albicans* (**b**), infected eye treated with INV/SNES system (**c**), infected eye treated with TZ suspension (**d**), agar dish cultivated with aqueous humor obtained from infected rabbits treated with INV/SNES system (**e**), and agar dish cultivated with aqueous humor obtained from infected rabbits treated with TZ suspension (**f**)

Figure 8a shows non-infected eyes without any abnormalities before induction of fungal infection. Upon induction of fungal infection, signs of keratitis were observed within 48 h, namely corneal ulcer, hypopyon, corneal vascularization, and corneal perforation as shown in Fig. 8b [26, 43]. Following treatment, the different animals in the different groups were observed and there was a marked difference between different groups. Most of the rabbits in group I (Fig. 8c), treated with TZ-loaded INV/SNES, showed rapid recovery rate within 5 days of treatment. Only one rabbit was recovered after 7 days of treatment. No mortality, hazardous clinical signs, nor adverse reactions were recorded in all animals in this group. Rabbits in group II, treated with TZ suspension, were not recovered throughout the 10-day period assigned for treatment. Furthermore, swelling of the infected eyes with scales and reactive corneal vascularization were observed (Fig. 8d). Clinical signs as well as adverse reactions were recorded in this group such as: off-food, depression, dropping head and ears, excessive slow movement, redness and milky discharge from rabbit's eyes.

Also, the aqueous humor of the different animals were collected after the assigned period of treatment and the microbiological count of *Candida albicans* was recorded after cultivation on Agar medium. Group I (Fig. 8e, treated with TZ-loaded INV/SNES), did not show any cultivated colonies indicating the absence of any *C. albican* cells in the aqueous humor following treatment, whereas the aqueous humor obtained from group II (treated with TZ suspension) showed a very high colony counts upon cultivation (Fig. 8f) which explain the inefficient treatment of this group.

Conclusion

In this study, we managed to prepare and optimize TZ-loaded BBNV with sustained TZ release profile and high residence time. The formulated system was investigated to assure its safety and low cytotoxicity compared to TZ suspension. Afterwards, this optimized system was integrated with a self-nanoemulsifying system in order to promote fast TZ release for the immediate antifungal activity, and to improve ocular residence and enhance TZ permeation to the inner corneal cells. The integrated system (INV/SNES) showed an optimum release profile which guarantee an effective inhibitory TZ level in the corneal cells, longer residence time, and subsequently, better antifungal activity. Thus, combining the dual mechanisms of both systems, SNES and BBNV could be a promising approach for ocular delivery of antifungal drugs for treatment of ocular fungal keratitis.

References

1. Thomas PA. Fungal infections of the cornea. Eye (London, England). 2003;17(8):852–62.
2. Kalkanci A, Ozdek S. Ocular fungal infections. Curr Eye Res. 2011;36(3):179–89.
3. O'Brien TP. Therapy of ocular fungal infections. Ophthalmol Clin N Am. 1999;12(1):33–50.
4. Kakkar S, Kaur IP. Spanlastics—a novel nanovesicular carrier system for ocular delivery. Int J Pharm. 2011;413(1):202–10.
5. Lakhundi S, Siddiqui R, Khan NA. Pathogenesis of microbial keratitis. Microb Pathog. 2017;104:97–109.
6. Peyton L, Gallagher S, Hashemzadeh M. Triazole antifungals: a review. Drugs Today (Barc). 2015;51(12):705–18.
7. Tolman E, Isaacson D, Rosenthale M, McGuire J, Van Cutsem J, Borgers M, et al. Anticandidal activities of terconazole, a broad-spectrum antimycotic. Antimicrob Agents Chemother. 1986;29(6):986–91.
8. Van Cutsem J, Van Gerven F, Zaman R, Janssen PAJ. Terconazole—a new broad-spectrum antifungal. Chemotherapy. 1983;29(5):322–31.
9. Schulman J, Peyman G, Dietlein J, Fiscella R, Colantino B. Ocular toxicity after intravitreal injection of terconazole. Ann Ophthalmol. 1989;21(9):345–7.
10. Bourlais CL, Acar L, Zia H, Sado PA, Needham T, Leverge R. Ophthalmic drug delivery systems—recent advances. Prog Retin Eye Res. 1998;17(1):33–58.
11. Ameeduzzafar, Ali J, Bhatnagar A, Kumar N, Ali A. Chitosan nanoparticles amplify the ocular hypotensive effect of cateolol in rabbits. Int J Biol Macromol. 2014;65:479–91.
12. Hironaka K, Inokuchi Y, Tozuka Y, Shimazawa M, Hara H, Takeuchi H. Design and evaluation of a liposomal delivery system targeting the posterior segment of the eye. J Control Release. 2009;136(3):247–53.
13. Aburahma MH. Bile salts-containing vesicles: promising pharmaceutical carriers for oral delivery of poorly water-soluble drugs and peptide/protein-based therapeutics or vaccines. Drug Deliv. 2016;23(6):1847–67.
14. Janga KY, Tatke A, Balguri SP, Lamichanne SP, Ibrahim MM, Maria DN, et al. Ion-sensitive in situ hydrogels of natamycin bilosomes for enhanced and prolonged ocular pharmacotherapy: in vitro permeability, cytotoxicity and in vivo evaluation. Artif Cells Nanomed Biotechnol. 2018;46(1):1039–50.
15. Abdelbary G. Ocular ciprofloxacin hydrochloride mucoadhesive chitosan-coated liposomes. Pharm Dev Technol. 2011;16(1):44–56.
16. Shamma RN, Elsayed I. Transfersomal lyophilized gel of buspirone HCl: formulation, evaluation and statistical optimization. J Liposome Res. 2013;23(3):244–54.
17. Basha M, Abd El-Alim SH, Shamma RN, Awad GE. Design and optimization of surfactant-based nanovesicles for ocular delivery of Clotrimazole. J Liposome Res. 2013;23(3):203–10.
18. Zeisig R, Shimada K, Hirota S, Arndt D. Effect of sterical stabilization on macrophage uptake in vitro and on thickness of the fixed aqueous layer of liposomes made from alkylphosphocholines. Biochim Biophys Acta Biomembr. 1996;1285(2):237–45.
19. Gonnissen Y, Gonçalves SI, De Geest BG, Remon JP, Vervaet C. Process design applied to optimise a directly compressible powder produced via a continuous manufacturing process. Eur J Pharm Biopharm. 2008;68(3):760–70.
20. Liu Z, Li J, Nie S, Guo H, Pan W. Effects of Transcutol P on the corneal permeability of drugs and evaluation of its ocular irritation of rabbit eyes. J Pharm Pharmacol. 2006;58(1):45–50.
21. Zhao Y, Wang C, Chow AH, Ren K, Gong T, Zhang Z, et al. Self-nanoemulsifying drug delivery system (SNEDDS) for oral delivery

of Zedoary essential oil: formulation and bioavailability studies. Int J Pharm. 2010;383(1–2):170–7.
22. Xue X, Cao M, Ren L, Qian Y, Chen G. Preparation and optimization of rivaroxaban by self-nanoemulsifying drug delivery system (SNEDDS) for enhanced oral bioavailability and no food effect. AAPS PharmSciTech. 2018;19(4):1847–59.
23. Yousry C, Zikry PM, Basalious EB, El-Gazayerly ON. Self-nanoemulsifying system optimization for higher terconazole solubilization and non-irritant ocular administration. Adv Pharm Bull, in press
24. Beg S, Swain S, Singh HP, Patra CN, Rao MB. Development, optimization, and characterization of solid self-nanoemulsifying drug delivery systems of valsartan using porous carriers. AAPS PharmSciTech. 2012;13(4):1416–27.
25. Wu TG, Wilhelmus KR, Mitchell BM. Experimental keratomycosis in a mouse model. Invest Ophthalmol Vis Sci. 2003;44(1):210–6.
26. Habib FS, Fouad EA, Abdel-Rhaman MS, Fathalla D. Liposomes as an ocular delivery system of fluconazole: in-vitro studies. Acta Ophthalmol. 2010;88(8):901–4.
27. Khan R, Irchhaiya R. Niosomes: a potential tool for novel drug delivery. J Pharm Investig. 2016;46(3):195–204.
28. Niu M, Tan Y, Guan P, Hovgaard L, Lu Y, Qi J, et al. Enhanced oral absorption of insulin-loaded liposomes containing bile salts: a mechanistic study. Int J Pharm. 2014;460(1–2):119–30.
29. Rajput T, Chauhan MK. Bilosome: a bile salt based novel carrier system gaining interest in pharmaceutical research. J Drug Deliv Sci Technol. 2017;7(5):4–16.
30. Aksungur P, Demirbilek M, Denkbas EB, Vandervoort J, Ludwig A, Unlu N. Development and characterization of cyclosporine A loaded nanoparticles for ocular drug delivery: cellular toxicity, uptake, and kinetic studies. J Control Release. 2011;151(3):286–94.
31. Fetih G. Fluconazole-loaded niosomal gels as a topical ocular drug delivery system for corneal fungal infections. J Drug Deliv Sci Technol. 2016;35:8–15.
32. Singh CH, Jain C, Kumar BN. Formulation, characterization, stability and invitro evaluation of nimesulide niosomes. Pharmacophore. 2011;3(3):168–85.
33. Wilkhu JS, McNeil SE, Anderson DE, Perrie Y. Characterization and optimization of bilosomes for oral vaccine delivery. J Drug Target. 2013;21(3):291–9.
34. Guan P, Lu Y, Qi J, Niu M, Lian R, Hu F, et al. Enhanced oral bioavailability of cyclosporine A by liposomes containing a bile salt. Int J Nanomedicine. 2011;6:965–74.
35. Müller R, Jacobs C, Kayser O. Nanosuspensions as particulate drug formulations in therapy: rationale for development and what we can expect for the future. Adv Drug Deliv Rev. 2001;47(1):3–19.
36. Dai Y, Zhou R, Liu L, Lu Y, Qi J, Wu W. Liposomes containing bile salts as novel ocular delivery systems for tacrolimus (FK506): in vitro characterization and improved corneal permeation. Int J Nanomedicine. 2013;8:1921–33.
37. Salama HA, Mahmoud AA, Kamel AO, Abdel Hady M, Awad GA. Brain delivery of olanzapine by intranasal administration of transfersomal vesicles. J Liposome Res. 2012;22(4):336–45.
38. Jovanović AA, Balanč BD, Ota A, Ahlin Grabnar P, Djordjević VB, Šavikin KP, et al. Comparative effects of cholesterol and β-sitosterol on the liposome membrane characteristics. Eur J Lipid Sci Technol. 2018;120(9):1800039.
39. Basalious EB, Shawky N, Badr-Eldin SM. SNEDDS containing bioenhancers for improvement of dissolution and oral absorption of lacidipine. I: development and optimization. Int J Pharm. 2010;391(1–2):203–11.
40. Basalious EB, El-Sebaie W, El-Gazayerly O. Application of pharmaceutical QbD for enhancement of the solubility and dissolution of a class II BCS drug using polymeric surfactants and crystallization inhibitors: development of controlled-release tablets. AAPS PharmSciTech. 2011;12(3):799–810.
41. Balakumar K, Raghavan CV, Abdu S. Self nanoemulsifying drug delivery system (SNEDDS) of rosuvastatin calcium: design, formulation, bioavailability and pharmacokinetic evaluation. Colloids Surf B Biointerfaces. 2013;112:337–43.
42. Singh SK, Verma PR, Razdan B. Glibenclamide-loaded self-nanoemulsifying drug delivery system: development and characterization. Drug Dev Ind Pharm. 2010;36(8):933–45.
43. Behrens-Baumann W, Klinge B, Rüchel R. Topical fluconazole for experimental candida keratitis in rabbits. Br J Ophthalmol. 1990;74(1):40–2.